Toxicon 101 (2015) 1–10

Contents lists available at ScienceDirect

Toxicon

journal homepage: www.elsevier.com/locate/toxicon

Post-transcriptional control of Amblyomin-X on secretion of vascular endothelial growth factor and expression of adhesion molecules in endothelial cells

C.C. Drewes [a], R.Y. Dias [a], V.G. Branco [b], M.F. Cavalcante [c], J.G. Souza [b], D.S.P. Abdalla [c], A.M. Chudzinski-Tavassi [b], S.H.P. Farsky [a, *]

[a] Laboratory of Experimental Toxicology, Department of Clinical and Toxicological Analyses, School of Pharmaceutical Sciences, University of São Paulo, Ave. Prof. Lineu Prestes 580, SP, 05503-900, São Paulo, Brazil
[b] Biochemistry and Biophysics Laboratory, Butantan Institute, Ave. Vital Brasil 1500, SP, 05503-900, São Paulo, Brazil
[c] Laboratory of Biochemistry, Department of Clinical and Toxicological Analyses, School of Pharmaceutical Sciences, University of São Paulo, Ave. Prof. Lineu Prestes 580, SP, 05503-900, São Paulo, Brazil

ARTICLE INFO

Article history:
Received 12 January 2015
Received in revised form
20 March 2015
Accepted 21 April 2015
Available online 22 April 2015

Keywords:
Dorsal chamber
Angiogenesis
β_3 integrin and VCAM-1
Amblyomma cajanense
Post-transcriptional control

ABSTRACT

Angiogenesis is a pivotal process of homeostasis and tissue repair, but it also favours neovascularisation syndromes and cancer nutrition. The chemical mediation of angiogenesis is complex, involving a balance between serine proteases and their inhibitors. We addressed the mechanisms of action of a Kunitz serine protease inhibitor (KPI) on spontaneous angiogenesis, using Amblyomin-X, a KPI designed from the cDNA library of the *Amblyomma cajennense* tick. Amblyomin-X treatment (10–1000 ng/10 μL; each 48 h; 3 times) reduced the number of vessels in the subcutaneous dorsal tissue of male Swiss mice, as measured by intravital microscopy, haematoxylin-eosin staining, and PECAM-1 immunofluorescence labeling. Incubation of Amblyomin-X with t-End endothelial cells, a murine endothelial microvascular lineage, did not alter cell proliferation, cell-cycle phases, necrosis and apoptosis, and the production of nitric oxide and prostaglandin E2. Nevertheless, Amblyomin-X treatment reduced t-End migration and adhesion to Matrigel®, and inhibited the VEGF-A secretion and VCAM-1 and β_3 integrin expressions by posttranscriptional pathways. Together, data herein outline novel posttranscriptional mechanisms of KPIs on endothelial cells during angiogenesis and point out the possible application of Amblyomin-X as a local inhibitor to undesired neovascularisation process.

1. Introduction

Angiogenesis is crucial from early embryonic to adult stages and to some adult physiological conditions, including cycling ovaries, placentation processes (Albrecht and Pepe, 2010), ventricular-subventricular zone neurogenesis (Sawada et al., 2014), and to the recovery of haemostasis during wound repair and tissue allograft transplantation (Wietecha and Dipietro, 2013). Nevertheless, enhanced angiogenesis is involved in the development of solid cancer by supplying nutrients for growth and metastasis (Welti et al., 2013), and in the severe neovascularisation syndromes associated with vision loss (Waltenberger, 2007; Baxter et al., 2013; Sawhney et al., 2013; Ergul et al., 2014), Alzheimer disease (Cameron et al., 2012; Huang et al., 2013; Ryu et al., 2013), and chronic rheumatoid arthritis (Shibuya, 2014; De Falco, 2014). Therefore, anti-angiogenic drug development relies on a knowledge of the molecular mechanisms controlling angiogenesis, which is pivotal in driving the advancement of specific therapeutic approaches (Goel and Mercurio, 2013; Welti et al., 2013; Kwaan et al., 2013).

Angiogenesis initiates with altered rheological parameters in the pre-existent blood vessel, characterised by enhanced vascular permeability and vasodilation, which favours the detachment of endothelial cells and their passage through the basement membrane. Subsequently, detached cells migrate and proliferate to form new outgrowths, which reorganise into a patent three-dimensional tubular structure of the new vessels (Risau, 1997). Endothelial cells must promptly answer to a gradient of chemical mediators to activate angiogenesis functions, and the fine balance of chemical

* Corresponding author.
E-mail address: sfarsky@usp.br (S.H.P. Farsky).

http://dx.doi.org/10.1016/j.toxicon.2015.04.002
0041-0101/

substances, secreted by different cells in the microenvironment, will orchestrate the process (Ferrara and Kerbel, 2005; Karamysheva, 2008; Shibuya, 2014).

A balance between serine proteases and their inhibitors is essential to haemostasis, including the control of angiogenesis (Masson, 2006; Rau et al., 2007). Inhibitors of serine proteases in stimulated angiogenesis, especially in cancer conditions, may cause anti- or pro-angiogenic effects (Murakami et al., 2010; Nishio et al., 2008; Fang et al., 2014). The controversial data may be due to the significant amount of overlapping mediators secreted in the tumour microenvironment, which may affect the serine protease/inhibitor balance (Kwaan et al., 2013). This is exemplified by the actions of the tissue factor pathway inhibitor 2 (TFPI- 2), the main KPI secreted by endothelial cells. TFPI-2 inhibits the proliferation, adhesion and migration of endothelial cells by impairing plasmin formation, reduces extravascular metalloprotease enzymes activities (Ivanciu et al., 2007), and impairs focal adhesion of endothelial cells to the extravascular matrix (Provençal et al., 2008). Moreover, TFPI-2 gene and protein expression is up-regulated by vascular endothelial growth factor-A (VEGF-A) actions (Xu et al., 2006). The latter effect has been proposed as a feedback mechanism that controls the pro-angiogenic actions of the growth factors (Xu et al., 2006).

Kunitz protease inhibitors (KPIs) comprise a class of peptides present in animals, plants and microorganisms, consisting of approximately 60 amino acid residues. These amino acids contain conserved cysteine residues forming three disulfide bridges, which confers the compact and stable nature of the folded polypeptide. KPIs may contain one or multiple Kunitz domains in a single-chain that interact with different proteases at their reactive sites (Ranasinghe and McManus, 2013). These characteristics, associated with a widespread but not uniform KPI expression in the tissues, lead to different actions of KPIs depending on the microenvironment of the angiogenesis process (Noel et al., 2004).

Animal venoms are an important source of KPIs, which have been employed as a scientific tool and are promising therapeutic approaches, especially for blood and vascular diseases (Chen et al., 2013). In this context, Amblyomin-X, a recombinant Kunitz-type FXa inhibitor (GenBank code AAT68575) identified in the transcriptome of the salivary glands of the *Amblyomma cajennense* tick (Batista et al., 2008, 2010) presents anti-tumour and anti-metastatic activities *in vivo* (Chudzinski-Tavassi et al., 2010; Ventura et al., 2013). Interestingly, our studies have demonstrated Amblyomin-X toxicity to tumour cells, but not to human fibroblasts, reinforcing its tissue-specific actions (Chudzinski-Tavassi et al., 2010; Maria et al., 2013). Moreover, we showed that Amblyomin-X inhibited the VEGF-A-induced angiogenesis in mice, by impairing the homotypic and heterotypic endothelial cell adhesion (Drewes et al., 2012).

Although Amblyomin-X has similarity to the endogenous tissue factor pathway inhibitor (TFPI), structural and molecular modelling studies showed that the pattern of charged residues in the Kunitz domain of Amblyomin-X was not similar to that in human TFPI-1 and TFPI-2, suggesting distinct functional features to the toxin (Pasqualoto et al., 2014). Therefore, to extend the knowledge of different KPIs on endothelial cell functions, and to further suggest Amblyomin-X as a promising scientific tool or even therapeutic agent, we here designed a set of *in vivo* and *in vitro* assays to show the molecular mechanisms of Amblyomin-X action on endothelial cell functions during angiogenesis.

2. Material and methods

2.1. Reagents

Monoclonal antibodies, Annexin-V and Matrigel® were purchased from BD PharMingen Technical (San Diego, CA, USA). Propidium iodide (PI), lipopolysaccharide *E.coli* (LPS) and Evans Blue were obtained from Sigma (St. Louis, Mo, USA). RPMI 1640 medium and fetal bovine serum (FBS) were purchased from Vitrocell (São Paulo, Brazil). The CellTrace CFSE cell proliferation kit was purchased from Invitrogen (NY, USA), the VEGF kit was purchased from Immuno-Biological Laboratories (Japan) and the PGE_2 kit was purchased from Cayman Chemical (Michigan, USA). Reagents for mRNA extraction and RT-PCR experiments were purchased from Invitrogen and Applied Biosystems, USA, respectively. Amblyomin-X was obtained according to Batista et al. (2010).

2.2. Animals

Male Swiss mice (25–30 g) were fed a standard pellet diet and water *ad libitum*, and anaesthetised with a mixture of ketamine(20 mg/kg, i.p.)and xylazine solution (2 mg/kg, i.p.) before each experimental procedure. All procedures were performed according to protocols approved by the Brazilian Society of Science of Laboratory Animals (SBCAL) for proper care and use of experimental animals and approved by the local ethical committee.

2.3. Cell culture

Polyoma middle T oncogene-transformed mouse endothelioma cells derived from the thymus (t-End; Willians et al., 1988) were cultured in RPMI 1640 supplemented with 10% fetal bovine serum (FBS) in a 5% CO_2, humidified atmosphere, at 37 °C. t-End cells were used at 3rd passage to *in vitro* studies.

2.4. Intravital microscopic assay: skinfold dorsal chamber

The skinfold dorsal chamber was implanted in male Swiss mice under anaesthesia as previously described by Harder et al. (2004). Amblyomin-X (10–1000 ng/10 μl) or saline (control) was topically applied. The treatment schedule was carried out on the 3rd, 5th and 7th days after chamber implantation. Animals were immobilised in a polycarbonate tube and the microcirculatory network visualised in the windows was photographed using a digital camera (Sony–Cyber-Shot – 7.2 Mega Pixels/Optical 3X, Japan) coupled to intravital microscopy equipment (Carl Zeiss, Germany). The images obtained before (day 3) and after the treatments (day 9) were quantified according to Dellian et al. (1996). Results are expressed as a percentage of the difference of the number of vessels before and after treatments in each group (n = 5–7 per group).

To confirm the presence of vessels in a vascular mesh, the skin was cut in sections (2–3 μm thick, paraffin embedded) and dyed with Haematoxylin and Eosin (H&E) solution or labelled with phycoeritrin monoclonal antibody anti-platelet-endothelial cell adhesion molecule-1 (PECAM-1-PE; CD 31, 1:100).

2.5. Vessel permeability assay

The effect of Amblyomin-X on vessel permeability was investigated according to Senger et al. (1990). Briefly, the animals were anaesthetised and Evans Blue dye (0.2 mL of 20 mg/kg) was injected intravenously via the tail vein. Five minutes later, the dorsal skin was shaved prior to the intradermal (i.d.) injection (maximum of six sites/mouse) of the saline or Amblyomin-X (10, 100 or 1000 ng/site). Thirty minutes after the i.d. injection of treatments, animals were sacrificed. Their dorsal skin was removed, and the injected sites were punched out and weighed. The vessel permeability was quantified by spectrophotometric measurement

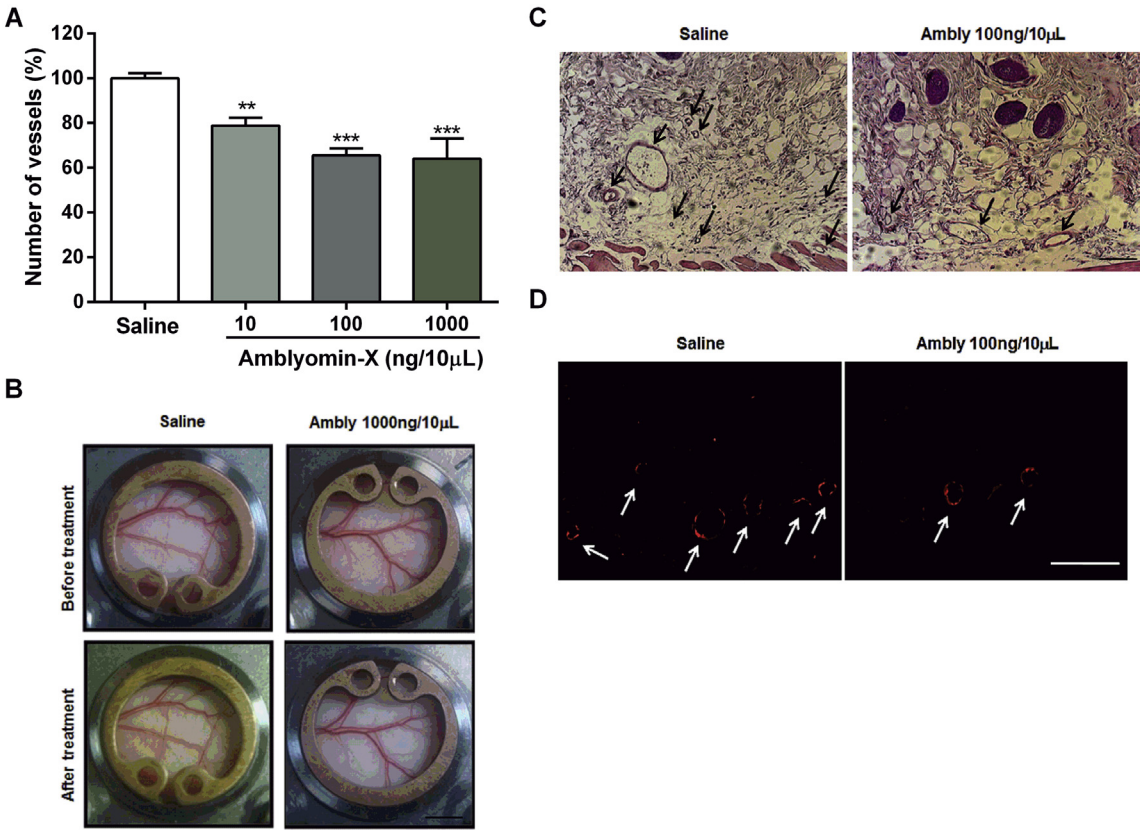

Fig. 1. Amblyomin-X reduces angiogenesis without any biological or chemical stimulation in dorsal chamber model. The mice were topically treated with Amblyomin-X (10, 100 or 1000 ng/10 μL) in the dorsal skin. The treatments were administrated once a day, at each 2 days, summarizing three applications (A). Representative images of dorsal skin were obtained before (day 3) and after (day 9) the treatments (B). Representative images of the dorsal skin stained with H&E (C; arrows indicate vessels) and vessels marked with anti-PECAM-1 (D; arrows indicate PECAM-1 staining) on vascular mesh in the end of treatments. Black bar = 100 μm. The results are expressed as the mean ± s.e.m. from three independent experiments. $^{**}p < 0.01$ and $^{***}p < 0.001$ compared with Saline group (ANOVA).

of the Evans blue dye extracted from skin sites. The values are expressed as the Optical Density (OD) = Absorbance $_{620nm}$ - Absorbance $_{690nm}$ x 100. The results are expressed as the OD percentage relative to the control group (n = 4–5 per group).

2.6. Flow cytometry: cell viability, cell proliferation and adhesion molecule expression

All experiments were conducted on a FACS Canto Flow Cytometer (Becton Dickinson, Mountain View, CA, USA) and analysed using the Flow Jo (version 9.1) software. Data from 10,000 events were obtained and only the morphologically viable endothelial cells were considered in the analysis.

To investigate the effect of Amblyomin-X on apoptosis and necrosis, Annexin-V-FITC and propidium iodide (PI) double staining was carried out. Cells were incubated with phosphate-saline buffer solution (PBS; control) or Amblyomin-X (100 or 1000 ng/mL) with culture medium supplemented with 10% of fetal bovine serum (FBS) for 72 h. At the end of the treatments, cells were incubated with Annexin-V-FITC (1:100) for 20 min at room temperature, PI (0.5 mg/tube) was added and flow cytometry analysis was immediately carried out. The results are expressed as the percentage of marked cells.

To investigate the effect of Amblyomin-X on cell proliferation, adherent cells were labelled with carboxyfluorescein diacetate succinimidyl ester (CFSE) according to the manufacturer's instructions. Briefly, the cells were washed with PBS and incubated with CFSE at a final concentration of 5 μM (37 °C for 15 min). Culture medium supplemented with 10% of FBS (1 mL) was added and the cells were incubated for 30 min. After the incubation, the cells were washed three times with PBS and incubated with PBS (control) or Amblyomin-X (10, 100 or 1000 ng/ml) for 24, 48 or 72 h. After the treatment period, cells were fixed and their fluorescence was analysed by flow cytometry. The results are expressed as fluorescence intensity and reductions in this parameter indicate an increment of cell proliferation.

The cell-cycle was evaluated in t-End cells incubated with PBS (control) or Amblyomin-X (100 ng/ml) for 24, 48 or 72 h. Afterwards, cells were washed with PBS, trypsinised and fixed by adding cold methanol (75%) for 1 h. DNA was stained with 200 μl of PI (10 μg/ml) and 20 μl of RNAse (15 μg/ml), and the percentage of cells in each phase of the cell cycle was determined.

The effect of Amblyomin-X on adhesion molecule expression of PECAM-1, VCAM-1, β_1 and β_3 integrin were evaluated on adhered cells into culture plate incubated with PBS (control) or Amblyomin-X (100 ng/ml) for 2 h. After this period, cells were removed and incubated with monoclonal antibody anti-PECAM-1 or anti-vascular cell adhesion molecule (VCAM-1) conjugated with PE or anti-β_1 integrin or anti-β_3 integrin conjugated with FITC, for 20 min at 4 °C in the dark. The results are expressed as the median of fluorescence intensity.

2.7. Cell adhesion assay

Adhered cells into culture plate (RPMI, FBS free) were incubated with PBS (control) or Amblyomin-X (10, 100 or 1000 ng/mL) for 2 h. Afterward, cells were removed using a cell scraper, and 5×10^4 cells were incubated on previously polymerised Matrigel®

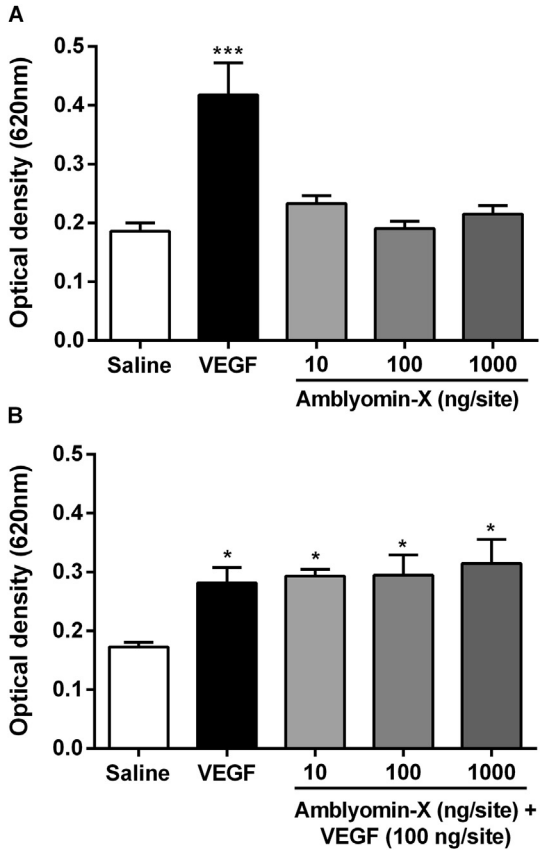

Fig. 2. Amblyomin-X does not alter vascular permeability *in vivo*. To evaluate the vascular permeability mice were subjected to intravenous injection of Evans blue dye, then the dorsal region, were performed intradermal injections of Saline, VEGF (100 ng/site, positive control) or Amblyomin-X (10, 100 or 1000 ng/site) (A) or co-treatment of Amblyomin-X plus VEGF (B). Treatment effects were assessed by quantifying the extravasated dye by spectrophotometry (620 nm). The results are expressed as the mean ± s.e.m. from four independent experiments. $^{*}p < 0.05$ and $^{***}p < 0.01$ compared with Saline group (ANOVA).

for 30 min at 37 °C. Cells were washed with PBS (2 ×) to remove non adherent cells and incubated with 0.1% crystal violet dye (100 μL) for 10 min at room temperature. The cells were washed (PBS; 4 ×) and fixed with acetic acid (50%; 100 μL) and the absorbencies were obtained at 580 and 690 nm. The values are expressed as the Optical Density (OD) = Absorbance $_{580\ nm}$ − Absorbance $_{690\ nm}$ × 100. The results are expressed as the OD percentage relative to the control group.

2.8. Cell migration assay

Confluent t-End cells (1×10^6) were cultured in a 12-well plate, and a "groove" in the centre of the well was wounded with a cell scraper (Burk, 1973). Afterwards, cells were gently washed once with PBS and incubated with PBS (control) or Amblyomin-X (10, 100 or 100 ng/mL) for 12 h. Cell migration was monitored with images obtained before and after the treatments using a digital camera coupled to a microscope (Nikon, magnification 1×). The number of cell nuclei that crossed the demarcated line was counted in three different microscopic fields.

2.9. Tube formation

The tube formation assay was performed on a Matrigel® layer. Briefly, Matrigel® was diluted in serum-free medium at a final concentration of 3 mg/ml, and 200 μl was added to each well and incubated at 37 °C for 1 h to form a gel layer. Subsequently, t-End cells (2×10^4/well) were incubated in 10% FBS-containing medium, in the presence or absence of Amblyomin-X (100 ng/mL) at 37 °C, in a humid atmosphere with 5% CO_2 for 8 h. Afterwards, cells were incubated in staining solution for 30 min at 37 °C, and the capillary-like structures formed in the gel were photographed (Axioskop II, Carl Zeiss, Germany) and the number of branches was quantified using Image J software.

2.10. Griess reaction

Endothelial cells (1×10^6) were incubated with Amblyomin-X (10, 100 or 1000 ng/mL) or PBS for 24 h. The amount of the stable metabolite NO_2^- in the culture supernatants was measured by a Griess reaction. Briefly, 100 μl of supernatant was incubated with 100 μl of Griess reagent (1% sulphanilamide solution and 0.1% a-naphthyl ethyl diamine solution) for 10 min. The absorbance was monitored at 550 nm using a multiwall plate reader (PowerWaveX340; Biotek Instruments, Inc.). The results are reported as μM of NO_2^-.

2.11. Immune assays

Endothelial cells (1×10^6) were incubated with PBS or Amblyomin-X (10, 100 or 1000 ng/mL) for 24 h to analyse the levels of VEGF and PGE_2. Concentrations of inflammatory mediators and growth factors were quantified in the supernatants using enzyme-linked immunosorbent assay (EIA) Kits according to the manufacturer's specifications and the results are expressed as pg/ml.

2.12. VCAM-1, β_3 integrin and VEGF mRNA expression

The t-End cells were incubated with PBS or Amblyomin-X (100 ng/mL) for 1 h and total RNA was isolated with TRIzol, and 2 μg of RNA was reverse-transcribed into cDNA using the SuperScript® VILO™ Master Mix (Invitrogen). Quantitative real-time PCR was performed in a 7500 Fast Real Time PCR System (Applied Biosystems) using Fast SYBR® Green PCR Master Mix and specific primer pairs for: VCAM-1 (sense: ACAGACAGTCCCCTCAATGG; anti-sense: ACCTCCACCTGGGTTCTCTT), β_3 integrin (sense: TGACATCGAGCAGGTGAAAG; anti-sense: GAGTAGCAAGGCCAATGAGC), VEGF-A (sense: TCACCAAAGCCAGCACATAG; anti-sense: TTTGACCCTTTCCCTTTCCT) and housekeeping gene RPL13a (ribosomal protein L13a) (sense: TCCTCAAGACCAACGGACTCCT; anti-sense: AACCTTTGGTCCCCACTTCCCT). The cycling program was 95 °C for 15 min, followed by 40 cycles of 95 °C for 15 s and 60 °C for 60 s. Each sample was run in duplicate. The expression of each target gene was normalised to RPL13a relative expression as an internal efficiency control. Values are reported as fold increase relative to the untreated control.

2.13. Statistical analyses

Means and standard error mean (s.e.m.) of all data are presented, which were compared by the Student's t-test or ANOVA, followed by Tukey's Multiple Comparisons. GraphPad Prism 5.0 software (San Diego, CA, USA) was employed. The differences were considered significant when p was less than 0.05.

3. Results

3.1. Effects of Amblyomin-X on in vivo angiogenesis in mice

The local *in vivo* angiogenic effects of Amblyomin-X on the

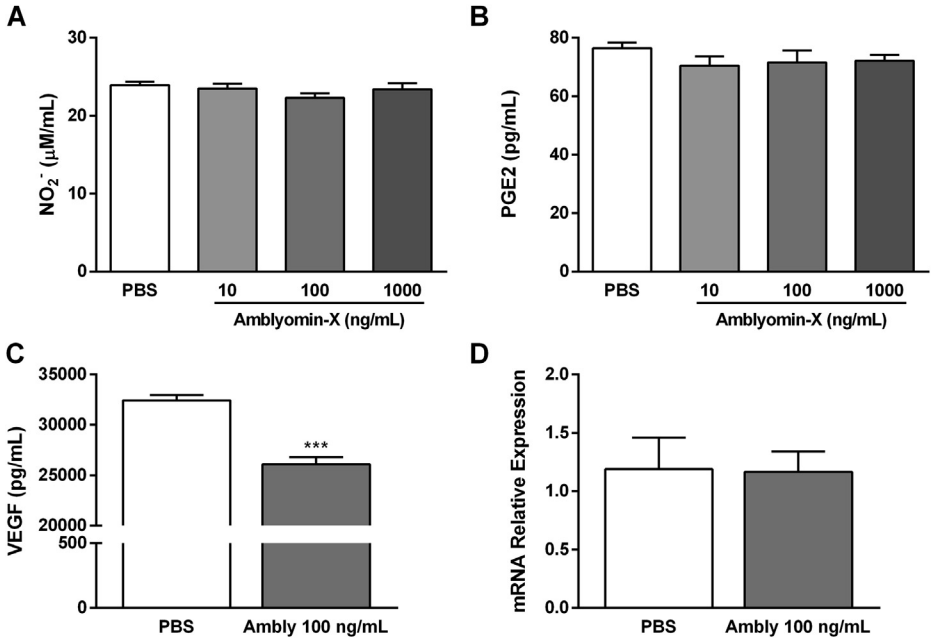

Fig. 3. Amblyomin-X does not alter levels chemical mediators and reduce levels of VEGF, without affect gene expression, by t-End cells. To evaluate the levels of NO (A), PGE2 (B) or VEGF (C) endothelial cells were cultured in the presence or absence of Amblyomin-X (10, 100 or 1000 ng/ml) during 24 h and supernatant was used to evaluate the levels of mediators by Griess reaction and enzyme-immunoassay, respectively. The VEGF mRNA produced by endothelial cells was evaluated by real time RT-PCR 1 h after treatments (D). The results are expressed as the mean ± s.e.m. from three independent experiments. ***$p < 0.001$ compared with PBS group (ANOVA or Student's t-test).

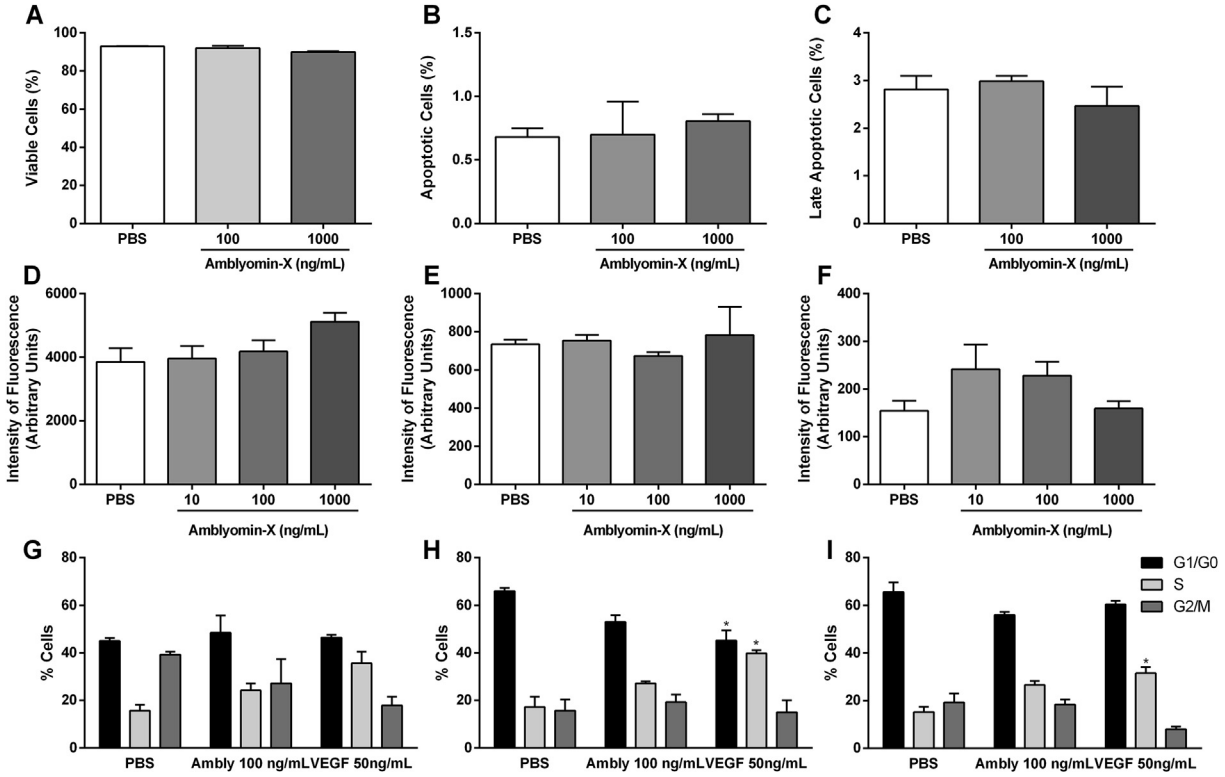

Fig. 4. Amblyomin-X does not alter endothelial cell viability, cell proliferation or cell cycle. Cells t-End was treated with PBS (control) or Amblyomin-X (10, 100 or 1000 ng/mL) and evaluated by flow cytometer. To evaluate the cell viability (A), apoptosis (B) and late apoptosis (C) the cells were treated (72 h) and incubated Anexin-V-FITC and PI (50 μg/ml, 10 μl/tube). To evaluate the cell proliferation, the cells were incubated with CFSE for 45 min and subsequently incubated with different treatments. The intensity of fluorescence was evaluated at 24 h (D), 48 h (E) or 72 h (F) after the treatments. To evaluate the cell cycle the t-End cells were incubated with different treatments for 24 h (G), 48 h (H) or 72 h (I) and labeled with PI (50 μg/mL). The results are expressed as the mean ± s.e.m. from three independent experiments (ANOVA).

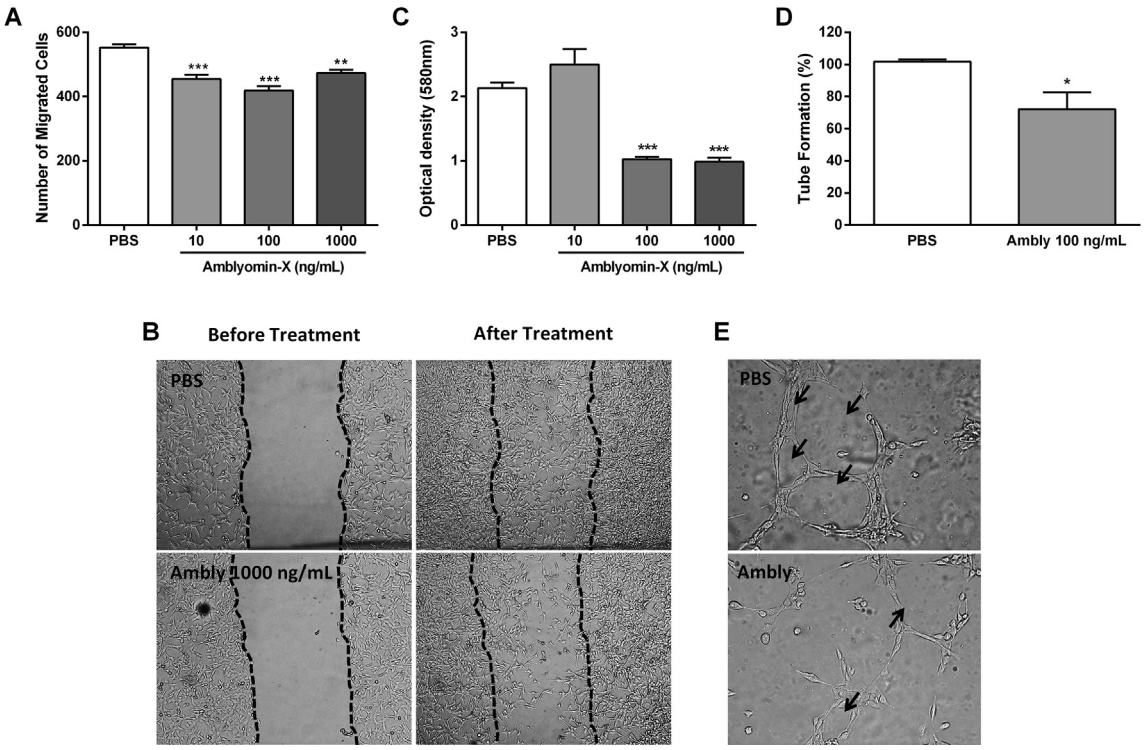

Fig. 5. Amblyomin-X inhibits endothelial cell adhesion, migration and tube formation. After t-End cells reached confluence it was wounded with a pipette tip, creating a "groove" in the center of well. Afterward, cells were incubated with PBS (control) or Amblyomin-X (10, 100 or 1000 ng/mL) during 12 h. The migration of the cells was monitored with images obtained before and after treatments (A, B). After t-End cells incubated with PBS (control) or Amblyomin-X (10, 100 or 1000 ng/mL) during 2 h, remained adhering for 30 min and were stained with crystal violet dye for 10 min. The adhesion cell on Matrigel® was monitored with absorbance (C). t-End cells were incubated with PBS or Amblyomin-X (100 ng/mL) on Matrigel® for 8 h and quantification of capillary-like structures was made using an optical microscope (D, E). Black bar = 100 μm. The results are expressed as the mean ± s.e.m. from three independent experiments. $^{*}p < 0.05$, $^{**}p < 0.01$, $^{***}p < 0.001$ compared with PBS group (ANOVA or Student's t-test).

dorsal subcutaneous tissue was measured by intravital microscopy, H&E staining, and PECAM-1 labelling. Data obtained showed that topical application of Amblyomin-X (10, 100 or 1000 ng/10 μL), each 48 h, significantly reduced the number of vessels in the subcutaneous tissue of mice compared to PBS treatment (Fig. 1A). The effect was not dose-dependent and the maximal inhibition on vessel formation was 35%. The representative images of *in vivo* angiogenesis obtained in intravital microscopy experiments, H&E staining of the vascular network and PECAM-1-labelled cells are shown in Fig. 1B, C and D, respectively.

3.2. Effects of Amblyomin-X on vascular permeability and secretion of chemical mediators

The intradermal (i.d.) injection of Amblyomin-X (10, 100 or 1000 ng/site) did not affect the microvascular permeability, as Evans blue extravasation into tissue was equivalent to that evoked by vehicle (PBS) injection (Fig. 2A). It is important to emphasise that intradermic injection of VEGF-A (100 ng/site), a known inducer of microvascular permeability and employed as positive controls for the experiment, significantly increased the microvascular permeability. Additionally, Amblyomin-X did not inactive VEGF-A, because the *in vivo* co-administration of VEGF-A and Amblyomin-X did not abolish the increased vascular permeability evoked by the growth factor (Fig. 2B).

Treatment of t-End endothelial cells with Amblyomin-X (10, 100 or 1000 ng/mL) did not alter the levels of NO and PGE_2 (Fig. 3A and B), which are involved in the *in vivo* enhanced vascular permeability during angiogenesis. The treatment of t-End cells with LPS (5 μg/mL) enhanced NO and PGE_2 levels in the supernatant, showing the efficacy of the experiment (NO: cells + PBS = 24 ± 0.4 μM/mL, cells + LPS: 166 ± 0.2 μM/mL; PGE_2: cells + PBS = 76.5 ± 2 pg/mL, cells + LPS: 455 ± 2.5 pg/mL).

In contrast, Amblyomin-X treatment reduced VEGF-A concentrations in the supernatant of endothelial cells (Fig. 3C), independently of gene expression, because VEGF-A mRNA levels were not reduced in Amblyomin-X-treated cells (Fig. 3D).

3.3. Effects of Amblyomin-X on endothelial cell viability, proliferation and cell cycle

The actions of Amblyomin-X on endothelial cell viability, proliferation and cycle were investigated using flow cytometry. Data presented in Fig. 4 shows that Amblyomin-X (100 or 1000 ng/mL) treatment did not cause apoptosis and late apoptosis (Fig. 4A–C). As positive control, cells were incubated with RPMI depleted serum (1%), which reduced about 40% of viable cells (2% apoptosis; 8% late apoptosis and 30% necrosis, data not shown).

Similarly, treatment with Amblyomin-X did not alter cellular proliferation measured after 24, 48 or 72 h (Fig. 4D–F) either induced cycle arresting measured until 72 h of incubation (Fig. 4G–I). Positive control was performed by incubating t-End with VEGF-A (50 ng/ml), which arrested the percentage of cells in phase S 48 h after incubation.

3.4. Effects of Amblyomin-X on endothelial cell adhesion, migration and tube formation

The role of Amblyomin-X during endothelial cell adhesion, migration and tube formation was assessed by spectroscopy and

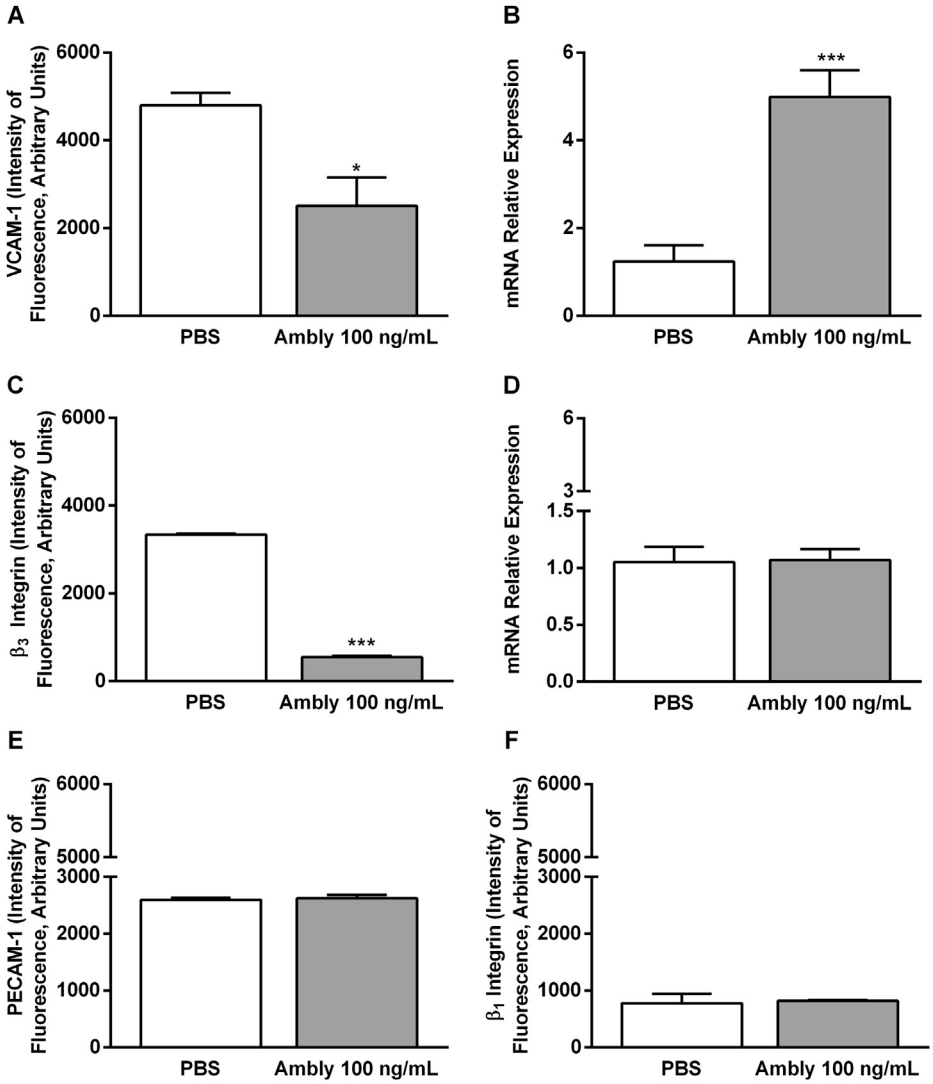

Fig. 6. Amblyomin-X inhibits expression of adhesion molecule VCAM-1 and β_3 integrin on endothelial cell but not inhibit mRNA expression. Endothelial cells were incubated with culture medium added of PBS (control) or Amblyomin-X (100 ng/mL) during 2 h to evaluate the expression of VCAM-1 (A), β_3 integrin (C), PECAM-1 (E) and β_1 integrin (F) by flow cytometry. The cells were incubated with treatments for 1 h to evaluate the levels of mRNA of VCAM-1 (B) and β_3 integrin (D) by real time RT-PCR. The results are expressed as the mean ± s.e.m. from three independent experiments. $^{*}p < 0.05$, $^{***}p < 0.001$ compared with PBS group (t-Test).

optical microscopy assays. Amblyomin-X (10–1000 ng/mL) treatments reduced cell migration (Fig. 5A and B) and adhesion in the Matrigel® matrix (10–1000 ng/mL; Fig. 5C). Nevertheless, it was not concentration related effect, as the reduction caused by 100 ng/mL was similar to that caused by 1000 ng/mL. In addition, analysis of tube formation showed that Amblyomin-X treatment (100 ng/mL) reduced the organisation of new vessels in the Matrigel® in t-End cells (Fig. 5D and E).

3.5. *Effects of Amblyomin-X on the expression of adhesion molecules in endothelial cells is independent of mRNA expression*

Based on the reduced adhesion and migration of endothelial cells after Amblyomin-X treatment, the effects of Amblyomin-X on the basal expression of adhesion molecules PECAM-1, VCAM-1, β_3 and β_1 integrins in endothelial cells were investigated using flow cytometry. The treatment with Amblyomin-X (100 ng/mL) reduced the expression of VCAM-1 (48 ± 13%) and β_3 integrin (83 ± 0.8%) (Fig. 6A and C). Amblyomin-X treatment did not alter PECAM-1 or β_1 integrin expression levels (Fig. 6E and F).

Real-time RT-PCR analysis showed that Amblyomin-X treatment increased the mRNA expression of VCAM-1 but not that of β_3 integrin (Fig. 6B and D, respectively).

4. Discussion

Therapeutic approaches for targeting complex processes such as angiogenesis require a fundamental understanding of the molecular control of cellular mechanisms. In this context, venom toxins have been employed as scientific tools to elucidate the molecular mechanisms regulating physiological and pathological conditions. Indeed, data here presented clearly show that the recombinant KPI protein Amblyomin-X alters post-transcriptional mechanisms in endothelial cells, which may be relevant for the impaired *in vitro* and *in vivo* angiogenesis caused by its local application.

Intravital microscopy has been highly utilised to evaluate tumour angiogenesis or that induced by exogenous chemical substances, as well as to evaluate the actions of anti-angiogenic agents (Drewes et al., 2012; Gellrich et al., 2014). Here, we evaluated the anti-angiogenic actions of Amblyomin-X in the absence

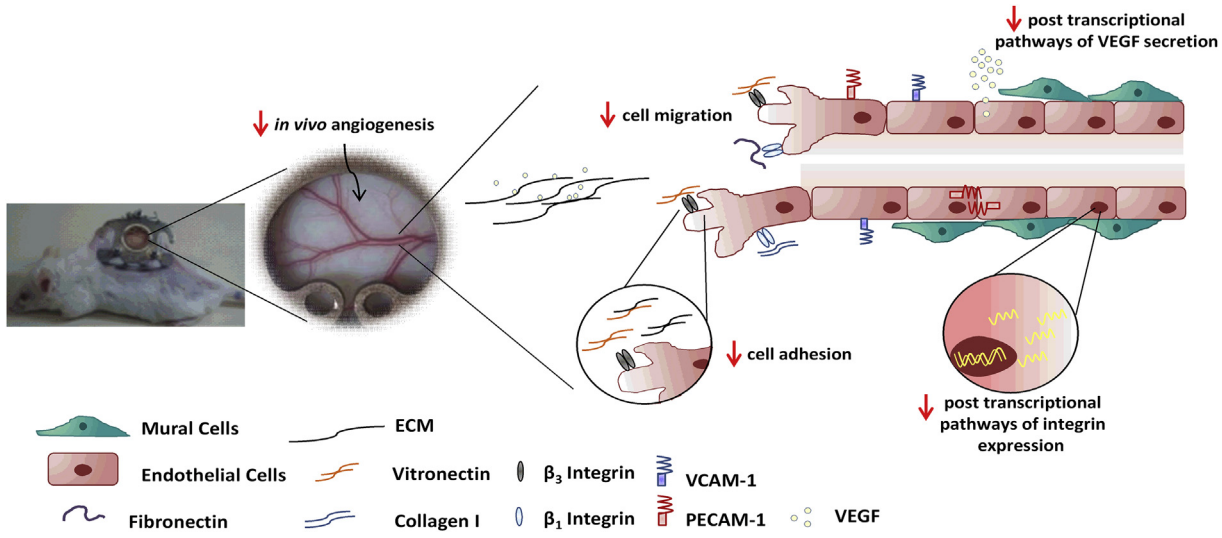

Fig. 7. Proposal pathway of Amblyomin-X actions on angiogenesis. Arrows indicate actions of Amblyomin-X on steps of angiogenesis process.

of any exogenous stimulation, except for that exerted by the surgical procedure to skinfold dorsal chamber implants. The inhibitory action of Amblyomin-X on vessel formation was confirmed by histological and immunofluorescence analyses. It is noteworthy to mention that PECAM-1 fluorescence labelling was crucial to indicate that the reduced number of vessels did not reflect an alteration of vessel rheology, as blood flow and vessel diameter, because PECAM-1 is constitutively expressed by endothelial cells and is used as a marker of vessel walls (Takase et al., 2013; Eman et al., 2014). In addition, Amblyomin-X treatment did not alter PECAM-1 expression by t-End cells, corroborating that PECAM-1 labelling is reliable for the analysis of vessel formation in the present study.

The observation that Amblyomin-X did not cause *in vivo* local alterations in vascular permeability reinforces that the protein does not present a direct action on endothelial contractile mechanisms. In addition, Amblyomin-X treatment did not affect the production of important inducers of vascular permeability, NO and PGE_2 by endothelial cells. Nevertheless, Amblyomin-X reduced VEGF-A secretion by a post-transcriptional mechanism. As VEGF-A is also a potent enhancer of vascular permeability (Shibuya, 2014), it may be suggested that the combination of endogenous vascular factors, such as histamine, serotonin, PGE_2 and NO, on angiogenesis may be responsible for the *in vivo* normal vascular permeability after Amblyomin-X injection. Additionally, co-administration of Amblyomin-X did not alter the enhanced vascular permeability evoked by exogenous administration of VEGF-A, indicating that Amblyomin-X does not modify the VEGF-A pathways responsible for endothelial cell contraction during the enhanced vascular permeability.

To our knowledge this is the first evidence for the post-transcriptional control of a KPI on VEGF-A secretion by endothelial cells. VEGF-A interacts with vascular endothelial growth factor receptors (VEGFRs 1 and 2) on cell membranes and triggers downstream intracellular mechanisms to physiological and pathological angiogenesis. VEGF-A induces endothelial permeability, proliferation, migration and adhesion during the process (Shibuya, 2014). Indeed, Amblyomin-X treatment reduced the adhesion and migration of endothelial cells; nevertheless, the direct actions of Amblyomin-X on endothelial cell adhesion and locomotion properties, or the dependence of reduced levels of VEGF-A caused by Amblyomin-X treatment remain to be clarified.

In vitro angiogenesis in a matrix mimetic system depends on homotypic and heterotypic endothelial cell adhesion. It is noteworthy to mention that the matrix system employed presents ligands to endothelial surface ligands, such as collagen, laminin and entactin. As different integrins subtypes bind into these ligands (Stupack and Cheresh, 2002, Weis and Cheresh, 2011; Plow et al., 2014), it may be supposed that Amblyomin-X may modulate the activities of these proteins or the expression of adhesion molecules in endothelial cells, reducing cell adhesion and tube formation process. Therefore, the role of Amblyomin-X on adhesion molecule expression in endothelial cells was further investigated. Indeed, Amblyomin-X treatment reduced the expression of VCAM-1 and β_3 integrin by t-End cells. VCAM-1 is linked to the endothelial–extravascular matrix and endothelial–leukocyte interactions (Schlesinger and Bendas, 2015; Kang et al., 2014), and β_3 integrin is a subfamily of heterodimers (of which $\alpha_v\beta_3$ integrin is the most important representative in the angiogenesis process) (Francavilla et al., 2009). The role of both VCAM-1 and $\alpha_v\beta_3$ integrin on angiogenesis has been fully shown by *in vitro* and *in vivo* molecular and pharmacological approaches (Schlesinger and Bendas, 2015; Kang et al., 2014). Recent data corroborate that KPI controls spontaneous angiogenesis, which may involve inhibitions of the expression and function of adhesion molecules. A KPI isolated from *Macrovipera lebetina* snake venom inhibited spontaneous human vascular endothelial cell adhesion, migration onto fibrinogen and fibronectin, and tube formation (Morjen et al., 2014). These effects depended on the instability of microtubule assembly, which may involve the interference with $\alpha_5\beta_1$ and $\alpha_v\beta_3$ integrin functions (Morjen et al., 2014).

The direct actions of KPIs on adhesion molecule expression is not fully understood, and our data highlight the post-transcriptional actions of Amblyomin-X on expression of VCAM-1 or β_3 integrin. This conclusion is reinforced by normal and elevated mRNA levels of VCAM-1 and β_3 integrin, respectively, and reduced protein expression of both adhesion molecules on cell membranes. The role of reduced secretion of VEGF-A after Amblyomin-X treatment on impaired adhesion molecule expression may not be ruled out, as both pre- and post-transcriptional pathways may be involved in VEGF-A-induced adhesion molecule expressions (Kim et al., 2003; Fearnley et al., 2014). Although the majority of data indicate the transcriptional control of VEGF-A on adhesion molecules, it has recently been shown that VEGF-A induces a direct interaction between the urokinase plasminogen activator receptor (uPAR) and integrins, leading to integrin

membrane redistribution and focal adhesion during angiogenesis. Reduced VEGF-A levels could impair uPAR-integrin interactions, reducing *in vitro* endothelial cell migration and *in vivo* angiogenesis (Alexander et al., 2012; Uhrin and Breuss, 2013; Montuori and Ragno, 2014). However, further studies are required to confirm the role of Amblyomin-X/VEGF-A/adhesion molecule expression in impaired angiogenesis.

In conclusion, data here highlight novel mechanisms of KPIs during the angiogenesis process, and implicate Amblyomin-X as a scientific tool for understanding the physiological and pathological pathways of vascular diseases (Fig. 7). Furthermore, our data emphasise that further studies must be carried out to validate the use of Amblyomin-X as a local therapeutic agent in aberrant neovascularisation syndromes.

Acknowledgements

The authors thank the financial support granted by Fundação de Amparo a Pesquisa do Estado de São Paulo (FAPESP 2008/57850-8; 2009/08584-6; 2008/56072-1, CeTICS-FAPESP 2013/07467-1) and Conselho Nacional de Pesquisa e Desenvolvimento (CNPq. INCTTOX). Carine C. Drewes is a PhD fellow from FAPESP (project 2010/19802-1), Rodrigo Dias was a graduate fellow from CAPES and Jean G. de Souza is a PhD fellow from FAPESP (project 2012/06944-8). Ana Marisa Chudzinski-Tavassi and Sandra H. P. Farsky are researcher fellows from Conselho Nacional de Pesquisa (CNPq).

Transparency document

Transparency document related to this article can be found online at http://dx.doi.org/10.1016/j.toxicon.2015.04.002.

References

Albrecht, E.D., Pepe, G.J., 2010. Estrogen regulation of placental angiogenesis and fetal ovarian development during primate pregnancy. Int. J. Dev. Biol. 54, 397–408.
Alexander, R.A., Prager, G.W., Mihaly-Bison, J., Uhrin, P., Sunzenauer, S., Binder, B.R., Schütz, G.J., Freissmuth, M., Breuss, J.M., 2012. VEGF-induced endothelial cell migration requires urokinase receptor (uPAR)-dependent integrin redistribution. Cardiovasc. Res. 94, 125–135.
Batista, I.F., Chudzinski-Tavassi, A.M., Faria, F., Simons, S.M., Barros-Batestti, D.M., Labruna, M.B., Leão, L.I., Ho, P.L., Junqueira-de-Azevedo, I.L., 2008. Expressed sequence tags (ESTs) from the salivary glands of the tick Amblyomma cajennense (Acari: Ixodidae). Toxicon 51, 823–834.
Batista, I.F., Ramos, O.H., Ventura, J.S., Junqueira-de-Azevedo, I.L., Ho, P.L., Chudzinski-Tavassi, A.M., 2010. A new factor Xa inibitor from Amblyomma cajannense with a unique domain composition. Arch. Biochem. Biophys. 493, 151–156.
Baxter, S.I., Pistilli, M., Pujari, S.S., Liesegang, T.I., Suhler, E.B., Thorne, Foster, C.S., Jabs, D.A., Levy-Clarke, G.A., Nussenblatt, R.B., Rosenbaum, J.T., Kempen, J.H., 2013. Risk of choroidal neovascularization among the uveitides. Am. J. Ophthalmol. 156, 468–477.
Burk, R.R., 1973. A factor from a transformed cell line that affects cell migration. Proc. Natl. Acad. Sci. U. S. A. 70, 369–372.
Cameron, D.J., Galvin, C., Alkam, T., Sidhu, H., Ellison, J., Luna, S., Ethell, D.W., 2012. Alzheimer's-related peptide amyloid-β plays a conserved role in angiogenesis. PLoS One 7, e39598.
Chen, Z., Cao, Z., Li, W., Wu, Y., 2013. Cloning and characterization of a novel Kunitz-type inhibitor from scorpion with unique cysteine framework. Toxicon 72, 5–10.
Chudzinski-Tavassi, A.M., De-Sá-Júnior, P.L., Simons, S.M., Maria, D.A., de Souza Ventura, J., Batista, I.F., Faria, F., Durães, E., Reis, E.M., Demasi, M., 2010. A new tick Kunitz type inhibitor, Amblyomin-X, induces tumor cell death by modulating genes related to the cell cycle and targeting the ubiquitin-proteasome system. Toxicon 56, 1145–1154.
De Falco, S., 2014. Antiangiogenesis therapy: an update after the first decade. Korean J. Intern. Med. 29, 1–11.
Dellian, M., Witwer, P.B., Salehi, A.H., Yuan, F., Jain, R.K., 1996. Quantitation and physiological characterization of angiogenic vessels in mice: effect of basic fibroblast growth factor, vascular endothelial growth factor/vascular permeability factor, and host microenvironment. Am. J. Pathol. 149, 59–71.
Drewes, C.C., Dias, R.Y., Hebeda, C.B., Simons, S.M., Barreto, S.A., Ferreira Jr., J.M., Chudzinski-Tavassi, A.M., Farsky, S.H., 2012. Actions of the Kunitz-type serine protease inhibitor Amblyomin-X on VEGF-A-induced angiogenesis. Toxicon 60, 333–340.
Ergul, A., Abdelsaid, M., Fouda, A.Y., Fagan, S.C., 2014. Cerebral neovascularization in diabetes: implications for stroke recovery and beyond. J. Cereb. Blood Flow. Metab. 34, 553–563.
Eman, R., Hoorntje, E.T., Oner, F.C., Kruyt, M.C., Dhert, W.J., Alblas, J., 2014. CXCL12/Stromal cell-derived factor-1 effectively replaces endothelial progenitor cells to induce vascularized ectopic bone. Stem Cells Dev. 23, 2950–2958.
Fang, B.A., Kovačević, Ž., Park, K.C., Kalinowski, D.S., Jansson, P.J., Lane, D.J., Sahni, S., Richardson, D.R., 2014. Molecular functions of the iron-regulated metastasis suppressor, NDRG1, and its potential as a molecular target for cancer therapy. Biochim. Biophys. Acta 1845, 1–19.
Fearnley, G.W., Odell, A.F., Latham, A.M., Mughal, N.A., Bruns, A.F., Burgoyne, N.J., Homer-Vanniasinkam, S., Zachary, I.C., Hollstein, M.C., Wheatcroft, S.B., Ponnambalam, S., 2014. VEGF-A isoforms differentially regulate ATF-2-dependent VCAM-1 gene expression and endothelial-leukocyte interactions. Mol. Biol. Cell. 25, 2509–2521.
Ferrara, N., Kerbel, R.S., 2005. Angiogenes is as a therapeutic target. Nature 438, 967–974.
Francavilla, C., Maddaluno, L., Cavallaro, U., 2009. The funtional role of cell adhesion in tumor angiogenesis. Semin. Cancer Biol. 19, 298–309.
Goel, H.L., Mercurio, A.M., 2013. VEGF targets the tumour cell. Nat. Rev. Cancer 13, 871–882.
Gellrich, D., Becker, S., Strieth, S., 2014. Static magnetic fields increase tumor microvessel leakiness and improve antitumoral efficacy in combination with paclitaxel. Cancer Lett. 343, 107–114.
Harder, Y., Amon, M., Erni, D., Menger, M.D., 2004. Evolution of ischemic tissue injury in a random pattern flap: a new mouse model using intravital microscopy. J. Surg. Res. 121, 197–205.
Huang, L., Jia, J., Liu, R., 2013. Decreased serum levels of the angiogenic factors VEGF and TGF-β1 in Alzheimer's disease and amnestic mild cognitive impairment. Neurosci. Lett. 550, 60–63.
Ivanciu, L., Gerard, R.D., Tang, H., Lupu, F., Lupu, C., 2007. Adenovirus-mediated expression of tissue factor pathway inhibits endothelial cell migration and angiogenesis. Arterioscler. Thromb. Vasc. Biol. 27, 310–316.
Kang, Z., Zhu, H., Luan, H., Han, F., Jiang, W., 2014. Corrigendum to curculigoside A induces angiogenesis through VCAM-1/EGR-3/CREB/VEGF signaling pathway. Neuroscience 267, 232–240.
Karamysheva, A.F., 2008. Mechanisms of angiogenesis. Biochemistry 73, 751–762.
Kim, W., Moon, S.O., Lee, S., Sung, M.J., Kim, S.H., Park, S.K., 2003. Adrenomedullin reduces VEGF-induced endothelial adhesion molecules and adhesiveness through a phosphatidylinositol 3'-kinase pathway. Arterioscler. Thromb. Vasc. Biol. 23, 1377–1383.
Kwaan, H.C., Mazar, A.P., McMahon, B.J., 2013. The apparent uPA/PAI-1 paradox in cancer: more than meets the eye. Semin. Thromb. Hemost. 39, 382–391.
Maria, D.A., de Souza, J.G., Morais, K.L., Berra, C.M., Zampolli, Hde C., Demasi, M., Simons, S.M., de Freitas Saito, R., Chammas, R., Chudzinski-Tavassi, A.M., 2013. A novel proteasome inhibitor acting in mitochondrial dysfunction, ER stress and ROS production. Invest New. Drugs 31, 493–505.
Masson, V., 2006. Roles of serine proteases and matrix metalloproteinases in tumor invasion and angiogenesis. Bull. Mem. Acad. R. Med. Belg. 161, 320–326.
Montuori, N., Ragno, P., 2014. Role of uPA/uPAR in the modulation of angiogenesis. Chem. Immunol. Allergy 99, 105–122.
Morjen, M., Honoré, S., Bazaa, A., Abdelkafi-Koubaa, Z., Ellafi, A., Mabrouk, K., Kovacic, H., El Ayeb, M., Marrakchi, N., Luis, J., 2014. PIVL, a snake venom Kunitz-type serine protease inhibitor, inhibits in vitro and in vivo angiogenesis. Microvasc. Res. 95C, 149–156.
Murakami, Y., Hosoi, F., Izumi, H., Maruyama, Y., Ureshino, H., Watari, K., Kohno, K., Kuwano, M., Ono, M., 2010. Identification of sites subjected to serine/threonine phosphorylation by SGK1 affecting N-myc downstream-regulated gene 1 (NDRG1)/Cap43- dependent suppression of angiogenic CXC chemokine expression in human pancreatic cancer cells. Biochem. Biophys. Res. Commun. 396, 376–381.
Nishio, S., Ushijima, K., Tsuda, N., Takemoto, S., Kawano, K., Yamaguchi, T., Nishida, N., Kakuma, T., Tsuda, H., Kasamatsu, T., Sasajima, Y., Kage, M., Kuwano, M., Kamura, T., 2008. Cap43/NDRG1/Drg-1 is a molecular target for angiogenesis and a prognostic indicator in cervical adenocarcinoma. Cancer Lett. 264, 36–43.
Noel, A., Maillard, C., Rocks, N., Jost, M., Chabottaux, V., Sounni, N.E., Maquoi, E., Cataldo, D., Foidart, J.M., 2004. Membrane associated proteases and their inhibitors in tumor angiogenesis. J. Clin. Pathol. 57, 577–584.
Pasqualoto, K.F., Balan, A., Barreto, S.A., Simons, S.M., Chudzinski-Tavassi, A.M., 2014. Structural findings and molecular modeling approach of a TFPI-like inhibitor. Protein Pept. Lett. 21, 452–457.
Plow, E.F., Meller, J., Byzova, T.V., 2014. Integrin function in vascular biology: a view from 2013. Curr. Opin. Hematol. 21, 241–247.
Provençal, M., Michaud, M., Beaulieu, E., Rivard, G.E., Béliveau, R., 2008. Tissue factor pathway inhibitor (TFPI) interferes with endothelial cell migration by inhibition of both the Erk pathway and focal adhesion proteins. Thromb. Haemost. 99, 576–585.
Ranasinghe, S., McManus, D.P., 2013. Structure and function of invertebrate Kunitz serine protease inhibitors. Dev. Comp. Immunol. 39, 219–227.
Rau, J.C., Beaulieu, L.M., Huntington, J.A., Church, F.C., 2007. Serpins in thrombosis, hemostasis and fibrinolysis. J. Thromb. Haemost. (Suppl. 1), 102–115.
Risau, W., 1997. Mechanisms of angiogenesis. Nature 386, 671–674.

Ryu, J.K., Little, J.P., Klegeris, A., Jantaratnotai, N., McLarnon, J.G., 2013. Actions of the anti-angiogenic compound angiostatin in an animal model of Alzheimer's disease. Curr. Alzheimer Res. 10, 252–260.
Sawada, M., Matsumoto, M., Sawamoto, K., 2014. Vascular regulation of adult neurogenesis under physiological and pathological conditions. Front. Neurosci. 53, 1–7.
Sawhney, G.K., Payne, J.F., Ray, R., Mehta, S., Bergstrom, C.S., Yeh, S., 2013. Combination anti-VEGF and corticosteroid therapy for idiopathic retinal vasculitis, aneurysms, and neuroretinitis syndrome. Ophthalmic Surg. Lasers Imaging Retina 44, 599–602.
Schlesinger, M., Bendas, G., 2015. Vascular cell adhesion molecule-1 (VCAM-1)-An increasing insight into its role in tumorigenicity and metastasis. Int. J. Cancer. 136, 2504–2514.
Senger, D.R., Connolly, D.T., Van de Water, L., Feder, J., Dvorak, H.F., 1990. Purification and NH2-Terminal amino acid sequence of Guinea pig tumor secreted vascular permeability Factor-1. Cancer Res. 50, 1774–1778.
Shibuya, M., 2014. VEGF-vegfr signals in health and disease. Biomol. Ther. (Seoul) 22, 1–9.
Stupack, D.G., Cheresh, D.A., 2002. Get a ligand, get a life: integrins, signaling and cell survival. J. Cell Sci. 115, 3729–3738.
Takase, Y., Tadokoro, R., Takahashi, Y., 2013. Low cost labeling with highlighter ink efficiently visualizes developing blood vessels in avian and mouse embryos. Dev. Growth Differ. 55, 792–801.
Uhrin, P., Breuss, J.M., 2013. uPAR: a modulator of VEGF-induced angiogenesis. Cell Adh. Migr. 7, 23–26.
Ventura, J.S., Faria, F., Batista, I.F., Simons, S.M., Oliveira, D.G., Morais, K.L., Chudzinski-Tavassi, A.M., 2013. A Kunitz-type FXa inhibitor affects tumor progression, hypercoagulable state and triggers apoptosis. Biomed. Pharmacother. 67, 192–196.
Waltenberger, J., 2007. New horizons in diabetes therapy: the angiogenesis paradox in diabetes: description of the problem and presentation of a unifying hypothesis. Immunol. Endocrinol. Metab. Agents Med. Chem. 7, 87–93.
Weis, S.M., Cheresh, D.A., 2011. αV integrins in angiogenesis and cancer. Cold Spring Harb. Perspect. Med. 1, a006478.
Welti, J., Loges, S., Dimmeler, S., Carmeliet, P., 2013. Recent molecular discoveries in angiogenesis and antiangiogenic therapies in cancer. J. Clin. Invest. 123, 3190–3200.
Wietecha, M.S., Dipietro, L.A., 2013. Therapeutic approaches to the regulation of wound angiogenesis. Adv. Wound Care 2, 81–86.
Willians, R.L., Courteneidge, S.A., Wagner, E.F., 1988. Embryonic lethalities an endothelial tumors in chimeric mice expressing polioma virus middle T oncogene. Cell 52, 121–131.
Xu, Z., Maiti, D., Kisiel, W., Duh, E.J., 2006. Tissue factor pathway inhibitor-2 is upregulated by vascular endothelial growth factor and suppresses growth factor-induced proliferation of endothelial cells. Arterioscler. Thromb. Vasc. Biol. 26, 2819–2825.